Direct estimation of the seismic demand and capacity of MDOF systems through Incremental Dynamic Analysis of an SDOF approximation

D. Vamvatsikos & C. A. Cornell
Department of Civil and Environmental Engineering Stanford University, Stanford, USA

ABSTRACT: Introducing a fast and accurate method to estimate the seismic demand and capacity of first-mode dominated multi-degree-of-freedom (MDOF) systems by approximating the Incremental Dynamic Analysis (IDA) through the Static Pushover (SPO) analysis. While the computer-intensive IDA would require several nonlinear dynamic analyses under multiple suitably-scaled ground motion records, the simpler SPO helps approximate the MDOF system with a single-degree-of-freedom (SDOF) oscillator whose backbone matches the structure's SPO curve far beyond its peak. Thanks to the empirical equations implemented in the SPO2IDA software, the summarized IDA curves of the resulting system are effortlessly generated, enabling an engineer-user to obtain accurate estimates of seismic demands and capacities for limit-states such as global dynamic instability. Using a nine-storey building as a case study, the methodology is favorably compared to the full IDA.

1 INTRODUCTION

At the core of Performance-Based Earthquake Engineering (PBEE) lies the accurate estimation of the seismic demand and capacity of structures, a task that several methods are being proposed to tackle. One of the promising candidates is IDA (Vamvatsikos & Cornell, 2002b), a computer-intensive procedure that has been incorporated in modern seismic codes (e.g. FEMA, 2000) and offers thorough demand and capacity prediction capability, in regions ranging from elasticity to global dynamic instability, by using a series of nonlinear dynamic analyses under suitably multiply-scaled ground motion records. Still, professional practice favors simplified methods, mostly using SDOF models that approximate the MDOF system's behavior by matching its SPO curve, coupled with empirical equations derived for such oscillators to rapidly obtain a measure of the seismic demand (FEMA, 1997). Such procedures could be extended to reach far into the nonlinear range and approximate the results of IDA, but for their using oscillators with bilinear backbones that only allow for elastic perfectly-plastic behavior, and occasionally positive or negative post-yield stiffness (e.g. Miranda, 2000, Nassar & Krawinkler, 1991). With the emergence of the SPO2IDA software (Vamvatsikos & Cornell, 2002a), empirical relations for full quadrilinear backbones are readily available, which, when suitably applied to the MDOF SPO, allow us to accurately approximate the full IDA and investigate the connection between the structure's SPO curve and its seismic behavior.

2 IDA FUNDAMENTALS

To illustrate our methodology, we will perform IDA for a centreline model of a 9-storey steel-moment resisting frame designed for Los Angeles according to the 1997 NEHRP provisions (Lee & Foutch, 2002). The model incorporates ductile members, shear panels and realistically fracturing Reduced Beam Section connections, while it includes the influence of interior gravity columns and a first-order treatment of global geometric nonlinearities (P-Δ effects). Essentially, it is a first-mode dominated structure that has its fundamental mode at a period of $T_1 = 2.3$ sec, accounting for 84.3% of the total mass, hence allowing for some significant sensitivity to higher modes.

We have also compiled a suite of twenty ground motion records that have been selected to represent a scenario earthquake (Vamvatsikos & Cornell, 2002c); the moment magnitude is within the range of 6.5–6.9, they have all been recorded on firm soil and show no directivity effects. IDA involves performing a series of nonlinear dynamic analyses for each record by scaling it to several levels of intensity that are suitably selected to uncover the full range of the model's behavior: from elastic to yielding and nonlinear inelastic, finally leading to global dynamic instability. Each dynamic analysis can be characterized by at least two scalars, an Intensity Measure (IM), which represents the scaling factor of the record (e.g. the 5%-damped first-mode spectral acceleration $S_a(T_1, 5\%)$) and a Damage Measure (DM), which monitors the structural response of the model (e.g. maximum peak

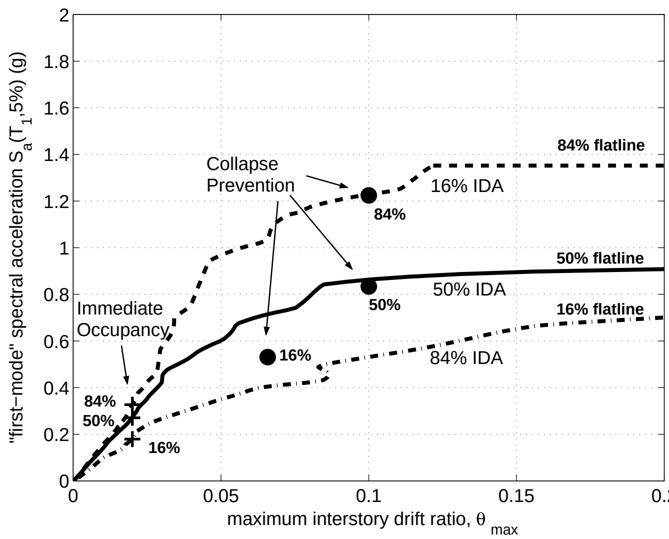

Figure 1. 16%, 50%, 84% fractile IDAs and limit-state capacities

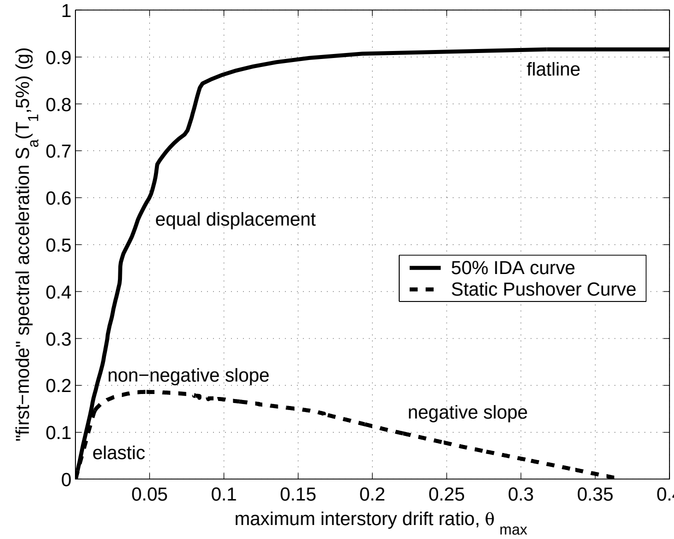

Figure 2. The median IDA compared against the SPO generated by an inverted-triangle load pattern

interstorey drift ratio θ_{max} or peak roof drift ratio θ_{roof}).

By suitably interpolating between the results of the dynamic analyses, we can plot on the *DM-IM* axes an IDA curve for each record. The twenty IDA curves that are thus produced can then be summarized into the 16%, 50% and 84% fractiles, as presented in Figure 1 and explained in detail by Vamvatsikos & Cornell (2002c). Additionally, limit-states such as Immediate Occupancy and Collapse Prevention (FEMA, 2000), or the global dynamic instability (evident by the characteristic flattening, termed the *flatline*, on each IDA) can be easily defined on the curves. Finally, by combining the results of IDA with a hazard analysis within a proper probabilistic framework, we can estimate the mean annual rates of exceeding each limit-state (Vamvatsikos & Cornell, 2002b), one of the ultimate goals of PBEE. Still, the calculation of the full, twenty-record IDA requires about 24 hours of computing on a single 1999-era processor, something that may be beyond the practicing engineer.

A path to a simpler solution appears if we choose to plot the SPO of the MDOF system on θ_{max} versus $S_a(T_1, 5\%)$ axes, where the total base shear is divided by the total mass and scaled to match the elastic part of the IDA by an appropriate factor (that is equal to one for SDOF systems). By thus plotting the SPO curve versus the median IDA curve on the same graph (Fig. 2), we observe that both curves are composed of the same number of corresponding and distinguishable segments (Vamvatsikos & Cornell, 2002b). The elastic segment of the SPO coincides by design with the elastic IDA region, having the same *elastic stiffness*, while the yielding and hardening of the SPO (evident by its non-negative slope up to the peak) forces the median IDA to approximately follow the familiar *equal displacement* rule for moderate period structures, by maintaining the same slope as in the elastic region. Past the peak, the SPO's negative stiffness appears as a characteristic flattening of the IDA, the flatline, that eventually signals global collapse when the SPO curve reaches zero strength. This apparent qualitative connection of the SPO and the IDA drives our research effort to provide a simple procedure that will use the (relatively easy-to-obtain) SPO plus some empirical quantitative rules to estimate the fractile IDAs for a given structure, providing the IDA curves at a fraction of the IDA computations.

3 SPO2IDA FOR SDOF SYSTEMS

Based on the established principle of using SDOF oscillators to approximate MDOF systems, we have investigated the SPO-to-IDA connection for simple oscillators. The SDOF systems studied were of moderate period with moderately pinching hysteresis and 5% viscous damping, while they featured backbones ranging from simple bilinear to complex quadrilinear with an elastic, a hardening and a negative-stiffness segment plus a final residual plateau that terminated with a drop to zero strength. The oscillators were analyzed through IDA and the resulting curves were summarized into their 16%, 50% and 84% fractile IDA curves which were in turn fitted by flexible parametric equations (Vamvatsikos & Cornell, 2002a). Having compiled the results into the SPO2IDA tool, available online (Vamvatsikos, 2001), an engineer-user is able to effortlessly get an accurate estimate of the performance of virtually any moderate-period oscillator without having to perform the costly analyses, almost instantaneously recreating the fractile IDAs in normalized coordinates of $R = S_a(T_1, 5\%)/S_a^y(T_1, 5\%)$ (where $S_a^y(T_1, 5\%)$ is the $S_a(T_1, 5\%)$-value to cause first yield) versus ductility μ.

4 SPO2IDA FOR MDOF SYSTEMS

Adopting an approach similar to FEMA 273 (FEMA, 1997) we can use the SDOF IDA results generated

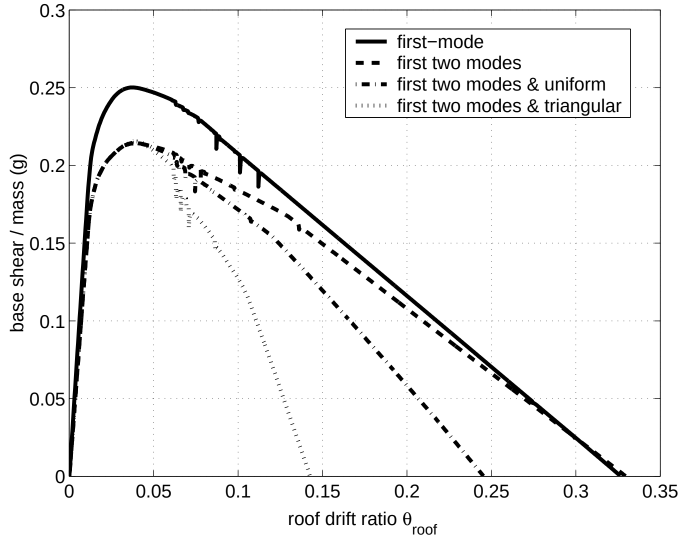

Figure 3. Four θ_{roof} SPOs produced by different load patterns.

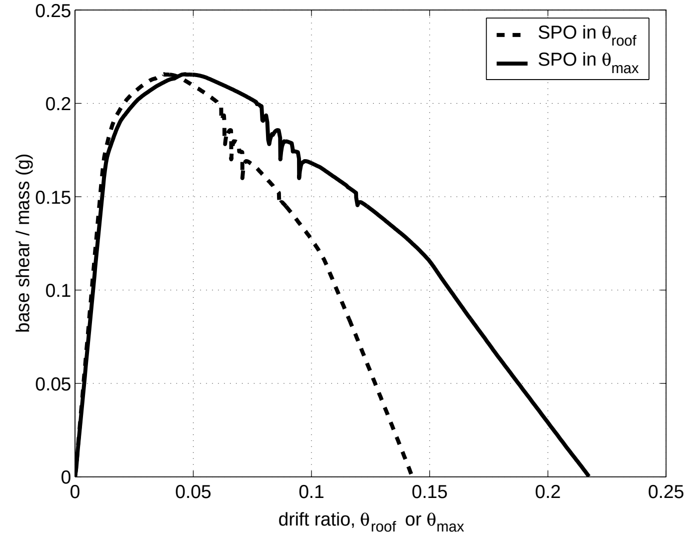

Figure 4. The most-damaging of the four SPO curves, shown in both θ_{roof} and $\theta_{\max}$ terms.

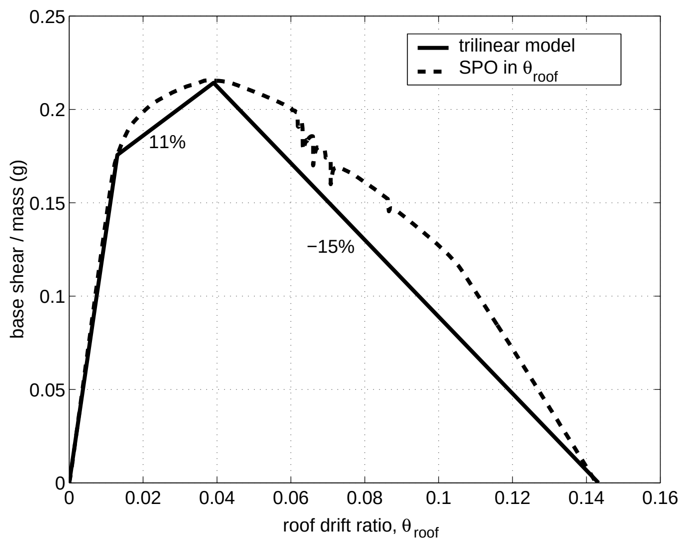

Figure 5. Approximating the most-damaging of the four θ_{roof} SPO with a trilinear model.

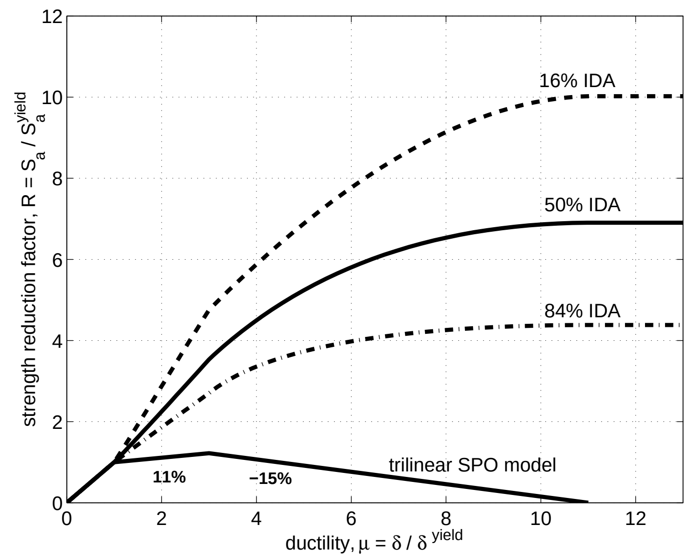

Figure 6. The fractile IDA curves for the SDOF with the trilinear backbone, as estimated by SPO2IDA.

by SPO2IDA to approximate the seismic behavior of the first-mode dominated MDOF system. This entails using an SDOF oscillator having the structure's fundamental period, whose backbone closely matches the SPO of the MDOF building. The resulting fractile IDA curves for the SDOF system only need to be properly rescaled from their R, μ coordinates to predict the fractile θ_{roof} IDAs and additionally, using the SPO, can be transformed to estimate the fractile $\theta_{\max}$ IDAs. While the methodology may seem straightforward, the ability of SPO2IDA to extend the results well into the SPO's post-peak region pushes the method to its limits and poses several challenges that have to be overcome.

4.1 *Defining the SPO*

While for an SDOF system the SPO is uniquely defined, this is not the case for the MDOF; depending on the load pattern selection, one may generate several different SPO curves, as evident in Figure 3. Therein we have plotted the θ_{roof} SPOs for the nine-storey building subjected to four different load patterns, producing four quite different SPOs. Beginning from the outermost SPO to the innermost, we observe the following:

1 A load pattern that is proportional to the first-mode shape times the storey masses is the most optimistic of the four, as it predicts the highest strength and roof drift ratio, $\theta_{\text{roof}} \approx 0.32$, before system collapse occurs.
2 If instead of just the first mode we use a Square-Root-Sum-of-Squares (SRSS) combination of the first two mode shapes we get the second most optimistic curve, where the maximum strength has dropped significantly, but the roof drift ratio at collapse remains $\theta_{\text{roof}} \approx 0.32$.
3 By changing the load pattern at the peak of the previous SPO to a uniform one, i.e. a shape that is directly proportional to the storey masses and resembles an SRSS of the first two mode shapes

of the damaged structure at the peak of the SPO, we uncover a severer drop towards collapse, with zero-strength occurring at $\theta_{\text{roof}} \approx 0.25$.

4 If instead of the uniform we impose in the post-peak region a triangular pattern (the minimum force being at the roof-level), it surprisingly produces the severest SPO of all, with global collapse happening at $\theta_{\text{roof}} \approx 0.14$, less than half of the prediction generated by the pure first-mode load pattern.

In essence, the choice of the load pattern has a significant effect on the calculated SPO curve and evidently, each of the four possible realizations pictured in Figure 3 will produce a different estimate for the seismic demands and capacities. As shown for simple oscillators by Vamvatsikos & Cornell (2002a), if we progress from the outermost SPO to the innermost one, the estimates of *DM* demands past the SPO peak will monotonically increase, and correspondingly the estimated *IM*-capacity for any limit-state that lies beyond the peak will decrease.

In general, the use of a rigid load pattern constrains the deformed shape of the structure, allowing it to withstand higher lateral loads and carry them to higher ductilities. Since structures usually collapse following a least-energy, least-resistance path, it makes sense to assume that a similar approach will render the best results for our approximating method, i.e. the SDOF oscillator whose backbone mimics the *worst-case* SPO will correctly approximate the dynamic behavior of the true MDOF model. Actually, we should expect that in the post-peak region, the further an SPO lies from the worst-case one, the more unconservative results it will produce, generating upper-bound estimates of limit-state capacities and lower-bound estimates of demands.

Such intuition is confirmed by comparing the deformed shapes of the structure produced by the various SPO and IDA curves. While the median IDA deformed shape shows that in the post-peak region most of the deformations are concentrated on the upper floors, only the most-damaging of the four SPOs manages to produce a similar deformation pattern. The other three load patterns seem to concentrate deformations mostly at the lower floors, thus not forcing the structure through the most-damaging, least-energy path as the dynamic analysis does. Hence, we choose to focus our efforts and all calculations to follow only on the most-damaging of the four SPOs.

Unfortunately there is no obvious recipe to help us arrive at the worst-case SPO. It is hard to predict in advance what load pattern will be the most appropriate, especially if one does not have a priori the dynamic analysis results to confirm that the dynamic and static deformed shapes match. Fully adaptive schemes may prove to be able to find the least-energy path to collapse, several candidates having been proposed at least by Gupta & Kunnath (2000) and Krawinkler & Seneviratna (1998), but none of the proposed schemes has been sufficiently tested and verified in the post-peak region, where good accuracy matters the most for all limit-states that lie close to global dynamic instability. A simpler, viable solution for regular structures involves using a pattern proportional to the SRSS of several mode shapes times the storey masses or a code-supplied pattern, at most up to the peak of the SPO (i.e. $\theta_{\text{roof}} \approx 0.02$ or $\theta_{\max} \approx 0.04$ in Figure 4), and consequently testing at least three configurations in the post-peak region : A triangle (maximum force at the first floor), a uniform and an inverted triangle (maximum force at the roof, i.e. almost a continuation of the pre-peak pattern). By performing these three basic pushovers we get sufficiently broad coverage and can pick a load pattern that will provide a good enough approximation to the overall most damaging, worst-case SPO.

Once we have an acceptable estimate of the worst-case θ_{roof} SPO, it is a simple matter to approximate it with a piecewise-linear backbone, in our case a trilinear elastic-hardening-negative model (Fig. 5), and process it through SPO2IDA. Instantaneously we will get estimates of the fractile IDAs for the SDOF with the matching trilinear backbone, as shown in Figure 6.

4.2 *Estimating the IDA elastic stiffness*

SPO2IDA will provide us with accurate estimates of the SDOF system fractile IDAs, but the results will be in dimensionless R versus μ coordinates, and need to be properly scaled to $S_a(T_1, 5\%)$ versus θ_{roof} or $\theta_{\max}$ axes. Therefore, we need to determine for each x%-fractile, $x \in \{16, 50, 84\}$, the values of $S_a(T_1, 5\%)$, θ_{roof} and $\theta_{\max}$ that correspond to its yield point, namely $S^y_{a,x\%}(T_1, 5\%)$, $\theta^y_{\text{roof},x\%}$ and $\theta^y_{\max,x\%}$. Obviously, for an SDOF system, the equivalent task is trivial, as the backbone directly provides us with the yield displacement and also the yield base shear, which when divided by the total mass will result to the value of $S^y_a(T_1, 5\%)$, common for all fractiles. This is much harder for an MDOF system, mainly due to the effect of the higher modes; some records will force the structure to yield earlier and some later, at varying levels of *IM* and *DM*. By assuming that the SPO accurately captures at least the median value $\theta^y_{\text{roof},50\%}$, the problem reduces to just estimating the elastic stiffness (*IM*/*DM*) of the median θ_{roof} and $\theta_{\max}$ IDA, or, even better, the elastic stiffness of all three fractile θ_{roof} and $\theta_{\max}$ IDAs, $k_{\text{roof},x\%}$ and $k_{\max,x\%}$ respectively.

Since such a task involves dynamic linear elastic analysis, there are several ways to perform it, a non-exhaustive list presented here in order of decreasing accuracy but increasing ease-of-computation:

1 Select a suitable suite of records and perform elastic response spectrum or timehistory analysis for each record to determine the peak roof and storey drifts. Directly estimate the 16%, 50% and 84% fractiles of the sample of elastic stiffnesses,

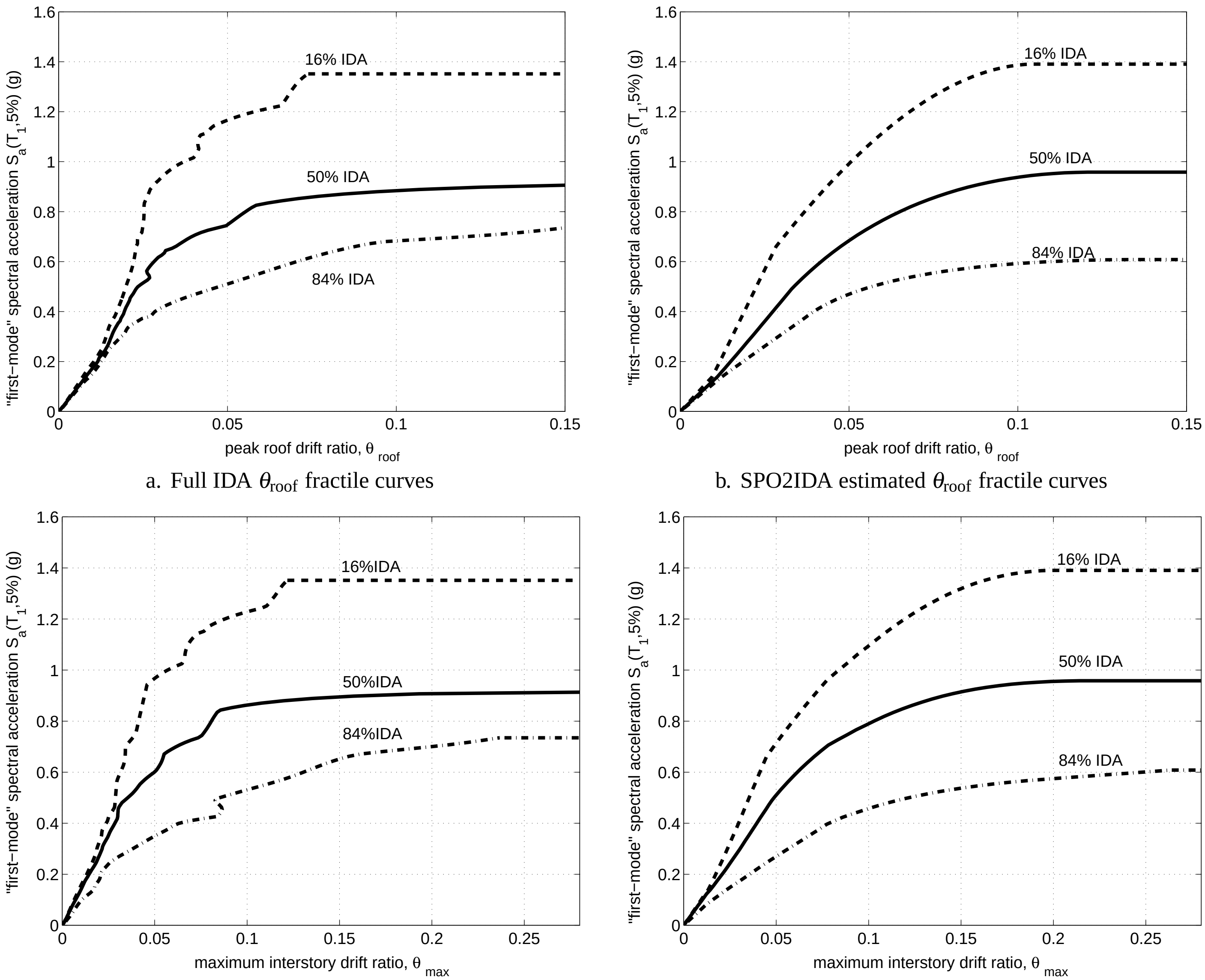

a. Full IDA θ_{roof} fractile curves

b. SPO2IDA estimated θ_{roof} fractile curves

c. Full IDA $\theta_{\max}$ fractile curves

d. SPO2IDA estimated $\theta_{\max}$ fractile curves

Figure 7. Generating the fractile IDAs from nonlinear dynamic analyses versus the MDOF SPO2IDA approximation.

$S_a(T_1, 5\%)/\theta_{\text{roof}}$ and $S_a(T_1, 5\%)/\theta_{\max}$, calculated for each ground motion.

2 Select a suitable suite of records, get their 16%, 50% and 84% spectra, perform response spectrum analysis for each and use the θ_{roof} and $\theta_{\max}$ elastic stiffness calculated as the 16%, 50% and 84% elastic θ_{roof} and $\theta_{\max}$ IDA stiffness respectively.

3 Using the median spectrum provided by the seismic code, perform response spectrum analysis. Use the calculated θ_{roof} and $\theta_{\max}$ elastic stiffness as an estimate for the median IDA θ_{roof} and $\theta_{\max}$ elastic stiffness. Assume no variability exists in the elastic stiffness, i.e. let $k_{\text{roof},x\%} = k_{\text{roof},50\%}$ and $k_{\max,x\%} = k_{\max,50\%}$

4 Approximate the median θ_{roof} and $\theta_{\max}$ elastic stiffness by dividing any elastic SPO level of base shear by the effective first-mode mass times the corresponding elastic θ_{roof} or $\theta_{\max}$ value respectively. Assume no variability exists in the elastic stiffness.

Although only the first method is an exact calculation of the elastic IDA stiffnesses, hence the method of choice for the calculations to follow, little accuracy is to be sacrificed if we use the simpler second method. The last two methods are useful mostly for shorter buildings with insignificant higher mode effects, since, in a manner similar to FEMA (1997), they neglect the variability in the elastic stiffness. Ultimately, the selection of the estimating procedure is a trade-off between speed and accuracy, and depends solely on each user's needs.

4.3 *Putting it all together*

Having determined the appropriate elastic stiffnesses for the fractile IDAs, all that remains is to properly de-normalize and scale the SPO2IDA results, from R versus μ coordinates, into $S_a(T_1, 5\%)$ versus θ_{roof} and $\theta_{\max}$ axes. Since the SPO has been approximated with a trilinear elastic-hardening-negative model (Fig. 5), yield-point values of base shear, θ_{roof} and $\theta_{\max}$, namely F^y, $\theta^y_{\text{roof,spo}}$ and $\theta^y_{\max,\text{spo}}$, are readily available. We will assume that each x%-fractile

IDA, $x \in \{16, 50, 84\}$, yields at about the same value of $S^y_{a,x\%}(T_1, 5\%)$, but at different $\theta^y_{\text{roof},x\%}$ and $\theta^y_{\max,x\%}$, hence we get:

$$S^y_{a,x\%}(T_1, 5\%) = \theta^y_{\text{roof,spo}} \cdot k_{\text{roof},50\%} \quad (1)$$

$$\theta^y_{\text{roof},x\%} = S^y_{a,x\%}(T_1, 5\%)/k_{\text{roof},x\%} \quad (2)$$

$$\theta^y_{\max,x\%} = S^y_{a,x\%}(T_1, 5\%)/k_{\max,x\%} \quad (3)$$

Using Equations 1–3, we can easily rescale the results of SPO2IDA and bring them in $S_a(T_1, 5\%)$ versus θ_{roof} axes to generate the θ_{roof} fractile IDAs, as seen in Figure 7b, which clearly compare very well against the real IDAs in Figure 7a.

If all that we want is an estimate of the *IM*-capacity for global dynamic instability of the structure, we need not proceed further. On the other hand, to estimate other limit-state capacities (e.g. Immediate Occupancy or Collapse Prevention), we need the IDAs expressed in other *DM*s, usually $\theta_{\max}$. The SPO curve actually provides the means for such a transformation thanks to the direct θ_{roof}-to-$\theta_{\max}$ mapping it establishes when expressed in θ_{roof} and $\theta_{\max}$ coordinates (Fig. 4), a concept that has been used at least in FEMA 273 (FEMA, 1997). The variation that we propose involves shifting the *DM* axis of the SPO for each x%-fractile, scaling the θ_{roof} values of the SPO by $\theta^y_{\text{roof},x\%}/\theta^y_{\text{roof,spo}}$ and the $\theta_{\max}$ SPO values by $\theta^y_{\max,x\%}/\theta^y_{\max,\text{spo}}$, thus providing a custom θ_{roof}-to-$\theta_{\max}$ mapping that will correctly transform demands for each fractile, recognizing the variability in elastic stiffness.

The results are visible in Figure 7d and compare favorably with the real IDA estimates in Figure 7c. Indeed, the estimated IDAs seem to slightly overestimate capacities and underestimate demands, mostly an effect of having just an approximation rather than the real worst-case SPO. Still, the approximation is good enough considering the $\pm 20\%$ bootstrap standard error that exists in estimating the fractiles from the twenty-record full IDA. Yet, regarding ease-of-computation, if we assume that a single 1999-era processor is used, the analysis time is reduced from 24 hours for the MDOF IDA, to only several minutes for the Static Pushover and the elastic response spectrum analyses not to mention the practically instantaneous SPO2IDA procedure. Thus, we have achieved a fast and inexpensive estimate of the MDOF dynamic behavior at only a little cost in accuracy, the results, at least for this structure, lying within the statistical error (caused by the record-to-record variability) of estimating the fractile IDAs from MDOF dynamic analyses.

5 CONCLUSIONS

A new approximate method for estimating the seismic demands and capacities of first-mode dominated structures has been presented. Based on the Static Pushover and building upon software able to accurately predict the Incremental Dynamic Analysis curves for SDOF systems, it can estimate, with reasonable accuracy, the fractile IDA curves of first-mode dominated MDOF systems. Several novel concepts are derived in the process, perhaps the most important being that of the worst-case, most-damaging SPO and its connection to the IDA. Using such an SPO curve plus a few elastic response spectrum analyses, the engineer-user is able to generate accurate predictions of the seismic behavior of complex MDOF structures within a fraction of the time needed for a full IDA.

6 ACKNOWLEDGEMENTS

Financial support for this research was provided by the sponsors of the Reliability of Marine Structures Affiliates Program of Stanford University.

REFERENCES

FEMA 1997. NEHRP guidelines for the seismic rehabilitation of buildings. *Report No. FEMA-273*, Federal Emergency Management Agency, Washington DC.

FEMA 2000. Recommended seismic design criteria for new steel moment-frame buildings. *Report No. FEMA-350*, SAC Joint Venture, Federal Emergency Management Agency, Washington DC.

Gupta, B. & Kunnath, S.K. 2000. Adaptive spectra-based pushover procedure for seismic evaluation of structures. *Earthquake Spectra* 16(2): 367–391.

Krawinkler, H. & Seneviratna, G.D.P.K. 1998. Pros and cons of a pushover analysis of seismic performance evalation. *Engineering Structures* 20(4-6): 452–464.

Lee, K. & Foutch, D.A. 2002. Performance evaluation of new steel frame buildings for seismic loads. *Earthquake Engineering and Structural Dynamics* 31(3): 653–670.

Miranda, E. 2000. Inelastic displacement ratios for structures on firm sites. *ASCE Journal of Structural Engineering* 126(10): 1150–1159.

Nassar, A.A. & Krawinkler, H. 1991. Seismic demands for SDOF and MDOF systems. *Report No. 95*, The John A.Blume Earthquake Engineering Center, Stanford University, Stanford.

Vamvatsikos, D. 2001. SPO2IDA: Moderate periods. URL `http://tremble.stanford.edu/cgi-bin/spo2ida-mt.pl`.

Vamvatsikos, D. & Cornell, C.A. 2002a. Direct estimation of the seismic demand and capacity of oscillators with multi-linear static pushovers through incremental dynamic analysis. In *Proceedings of the 7th U.S. National Conference on Earthquake Engineering*, Paper No. 354. Boston, MA: EERI, El Cerrito, CA.

Vamvatsikos, D. & Cornell, C.A. 2002b. Incremental dynamic analysis. *Earthquake Engineering and Structural Dynamics* 31(3): 491–514.

Vamvatsikos, D. & Cornell, C.A. 2002c. The incremental dynamic analysis and its application to performance-based earthquake engineering. In *Proceedings of the 12th European Conference on Earthquake Engineering*, Paper No. 479. London, UK.